Journal of Dental Sciences (2018) 13, 267–273

Available online at www.sciencedirect.com

ScienceDirect

journal homepage: www.e-jds.com

Original Article

The effect of plasma treatment on the osseointegration of rough titanium implant: A histo-morphometric study in rabbits

Wan-Ching Chou [a], Rex C.-C. Wang [a], Chih-Ling Huang [b], Tzer-Min Lee [c,d*]

[a] Institute of Manufacturing Information and Systems, National Cheng Kung University, Tainan, Taiwan
[b] Center for Fundamental Science, Kaohsiung Medical University, Kaohsiung, Taiwan
[c] Institute of Oral Medicine, National Cheng Kung University Medical College, Tainan, Taiwan
[d] School of Dentistry, Kaohsiung Medical University, Kaohsiung, Taiwan

Received 21 April 2018; Final revision received 28 May 2018
Available online 19 June 2018

KEYWORDS
Hydrophilicity;
Functional OH groups;
Plasma treatment;
Bone-to-implant contact

Abstract *Background/purpose:* The surface properties, such as hydrophilicity and functional OH groups, play an important role in bone fixation *in vivo*. In our previous study, the plasma treatments of large grit and acid etching (SLA) method produce functional OH groups on the rough surface. There is no report in discussing the integration between basic Ti–OH groups and bone-to-implant contact (BIC). The aim of this study was to evaluate the effect of the functional OH groups on the rough surface both *in vitro* and *in vivo*.
Materials and methods: Functional hydroxyl groups were produced on a SLA-treated surface. The surface topography, roughness, wettability, and chemical composition were examined using various techniques. Twenty-four implants were inserted into the proximal tibia of four New Zealand white rabbits. The biological responses were measured in terms of histomorphometric analysis 4 and 8 weeks post-implantation.
Results: The surface morphology and roughness were similar among all groups. However, the concentration of OH groups and hydrophilicity were found increased in the plasma treatment. The cell morphology in RF-plasma treated groups had more polygonal type and higher expression of actin and vinculin. The bone-to-implant contact (BIC) ratios of RF-200W were significantly higher than other groups ($P < 0.05$). The relationship between basic OH groups and BIC showed linear correspondence.
Conclusion: The Ti–OH groups introduced on the rough surface by plasma treatments can trigger cell adhesion which further initiate new bone apposition. We propose that RF-plasma treatment can help to enhance bone healing at 4 and 8 weeks.

* Corresponding author. 1 University Road, Tainan, 701, Taiwan. Fax: +886 6 2095845.
E-mail address: tmlee@mail.ncku.edu.tw (T.-M. Lee).

https://doi.org/10.1016/j.jds.2018.06.002

Introduction

Artificial implants with good osseointegration is an important factor in the success of implantation. Osseointegration refers to bone-implant interface bonding. Direct contact between an implant and surrounding bone often depends on the implant surface properties.[1–3] Sand-blasting with large grit and acid etching (SLA) is commonly used as a surface treatment because it produce a high contact ratio with micron and submicron roughness surface.[4] SLA is often used in commercial implant surface treatment; however, since bone healing time takes about 8 weeks, the surface properties need to be further optimized. Compared with SLA treated implants, those with chemically modified SLA (modSLA) can reduces healing time to 3–4 weeks because the surface becomes more hydrophilic.[5] Therefore, to speed up osseointegration, plasma treatment can be considered SLA-implant surfaces to introduce functional groups and enhance hydrophilicity.

Study have shown that hydrophilic SLA surface influence osteoblast behavior by altering protein absorption and focal adhesion, which can directly induce cell differentiation through a subsequent intracellular signaling cascade.[6] Additional surface plasma treatment showed many advantages like introduce functional groups, change wettability, and eliminate contamination, making it an ideal and effective modification method for improving physicochemical properties.[7] The amount of surface hydroxyl $(OH)_s$ groups that contains acidic OH groups and basic OH groups increased by plasma treatment; such groups are a key factor in osteoblast–titanium interaction.[8] After plasma treatment, the surface becomes hydrophilic and contains abundant hydroxyl OH groups. Cells live on the OH-rich surface exhibit excellent growth and differentiation.[9–11] Canullo et al. reported that plasma treatment can improve protein adsorption and cell adhesion on a rough titanium substrate.[12] MacDonald et al. used radio-frequency plasma treatment to increase shear strength (determined using a pull-out test) and increase implant-femur bonding.[13]

The success of a clinical implant is mainly determined by the bonding strength and osseointegration between the implant and new surrounding bone tissues.[14] In our previous study, the plasma treatments of large grit and acid etching (SLA) method produced functional OH groups on the rough surface. Since there is no report in discussing the integration between basic Ti–OH groups and bone-to-implant contact (BIC). The present study uses simple and quick plasma treatment to introduce functional OH groups onto an implant surface and examines the cell cytoskeleton *in vitro* and bone-to-implant contact *in vivo*. The surface properties of plasma- and SLA-treated samples were also examined. Cell adhesion was investigated *in vitro* using immunofluorescence staining. Finally, bone-to-implant contact was measured to evaluate bone healing in a rabbit model.

Materials and methods

Sample preparation

Commercially pure Ti discs (cpTi, ASTM F67, Grade II) measuring 12.7 mm in diameter and 2 mm in thickness were used *in vitro*. A pure titanium implant measuring 11.52 mm in length and 2.48 mm in diameter and with a small head was used *in vivo*. The discs and implants were sand-blasted with large grit Al_2O_3 (particle size: 355–425 μm) at a pressure of 4 kg/cm^2. Then, a mixed acid (HCl/H_2SO_4 in ratio of 1:3) was used to treat the samples for 30 min at 80 °C. The samples were then washed with acetone, ethanol, and distilled water in sequence.

Plasma treatments

The SLA-treated samples (flat specimens and implants) were separately modified using plasma treatments under an atmosphere of oxygen. The DC and RF plasma treatment procedures followed those reported in a previous study.[11] The plasma-treated specimens were placed in the oxygen atmosphere for more than 10 min and then used absolute alcohol to keep its original properties before being analyzed.

The samples are denoted as follows: control (only SLA), DC-50W (SLA-treated titanium treated using DC plasma at 50 W), RF-50W (SLA-treated titanium treated using RF plasma at 50 W), and RF-200W (SLA-treated titanium treated using RF plasma at 200 W). The wettability, functional OH groups, and protein adsorption values are listed in Table 1.[11] The surface roughness was evaluated using a surfcorder (SE 1200; Kosaka Laboratory Ltd., Japan). The surface morphology was examined using scanning electron microscopy (SEM, JSM-6390LV, JEOL, Japan).

Cell cytoskeleton development

A fluorescence microscope (LSM780, Zeiss, Germany) was used to observe the cell morphology and cytoskeletal distribution. Cells were cultured at a seeding density of 5×10^3 cells/cm^2 on the specimens (four groups). Vinculin was stained using a mouse monoclonal antibody (Sigma, USA) and anti-mouse IgG conjugated with Alexa fluor 594 (Molecular Probes, USA). F-actin was labeled with Alexa fluor 488-labled phalloidin (Molecular Probes, USA). The samples were stained with 4',6-diamidino-2-phenylindole dihydrochloride (DAPI) nuclear dye and finally fixed using ProLong® Gold antifade reagents (Molecular Probes, USA) before fluorescence microscopy analysis.

Table 1 Surface characteristics of control, DC-50W, RF-50W, and RF-200W (n = 5).

	Roughness (μm)	Contact angle (°)	XPS analysis[a]			Protein adsorption[a] (μg)
			Basic Ti—OH (%)	Acidic OH (%)	O1s (%)	
Control	2.63 ± 0.25	112 ± 6	10.00	8.21	81.79	0.23
DC-50W	2.57 ± 0.28	<10	19.08	29.80	51.12	0.26
RF-50W	2.81 ± 0.17	<10	21.91	25.70	52.39	0.34
RF-200W	2.71 ± 0.34	<10	33.05	23.86	43.09	0.47

[a] From our previous study.[11]

Animals and surgical procedure

The animal experiment followed the animal approval (IACUC #103305) of National Cheng Kung University (Tainan, Taiwan). Four adult male New Zealand white rabbits weighing 3.0—3.5 kg were used in this study. The surgical process was based on that published in a previous study.[15] The animals were anesthetized intramuscularly with a mixture of tiletamine/zolazepam (Zoletil, Virbac, France) and xylazine (Rompun, Bayer, USA). Three implants were implanted into each tibia. All implants were inserted through the first cortical layer. After surgery, all the rabbits were injected with topical analgesics and antibiotics. All the animals were kept in individual cages in the animal experiment center of National Cheng Kung University. They were given the standard laboratory diet. 4 or 8 weeks post-implantation, the rabbits were given an overdose of tiletamine/zolazepam (Zoletil) (10 ml, i.m.); the rabbits were then euthanized using potassium chloride (10 ml, i.m.). Two rabbits were euthanized for each time period (4 and 8 weeks).

Histological and histomorphometric evaluations

After the animals were euthanized, the tibia of two rabbits were removed at the specified time periods for histomorphometric analysis. The sample preparation protocol followed Lillie's method.[16] Histomorphometric analysis was conducted and bone-to-implant contact (BIC) ratio was calculated based on backscattered electron image of scanning electron microscopy BEI-SEM (JSM-6390LV, JEOL, Japan). The BIC ratio (%) was calculated by dividing the length from implant head edge to the second thread by the distance of the bone in direct contact with the implant surface. The BIC ratio of the implant was calculated using the software Image J (National Institutes of Health, USA) after image processing.

Statistical analysis

The BIC data are shown as means ± standard deviation (SD). Significant differences between control, DC plasma treatment, and RF plasma treatment groups were determined using one-way analysis of variance (ANOVA). The data were evaluated using Statistical Analysis System software (SAS; SAS Institute Inc., Cary, NC, USA). Results were considered significant at $P < 0.05$. The Duncan test was used to determine the significance level to specify treatment effects.

Results

Surface characterization

Fig. 1 SEM images showed all samples have the similar surface structure, namely a mountain and valley structure with micron- and submicron-scale notches. The morphology was the same for all groups and the surface roughness values, determined by the surfcorder, showed no statistically difference ($P > 0.05$). Wettability was estimated using the contact angle test. The mean contact angle of the control was 112°; a contact angle of over 90° indicates hydrophobicity. The plasma-treated samples had a contact angle of 0° (see Fig. 1), indicating that they were hydrophilic (Table 1). The OH group ratios, determined using X-ray photoelectron spectroscopy (XPS), were cited from our previous study[11] (see Table 1). Result showed that the basic Ti—OH ratio increased as plasma power increase. RF-200W had the highest basic OH ratio among the four groups. The acidic OH content increased after DC or RF plasma treatment. RF-200W had the highest OH group content. In this study, DC and RF plasma samples with various OH group content levels were used to examine the effect of functional OH groups *in vitro* and *in vivo*.

Cell adhesion and spreading examined using immunofluorescence

A fluorescence microscope was used to examine cell morphology and cytoskeletal organization. MG63 cells fluorescence images cultured on the four kinds of specimen for 1 and 24 h are shown in Figs. 2 and 3, respectively. The cells show the complex focal adhesion characteristic pattern with dense phalloidin-stained f-actin (green) and vinculin (red).

After 1 h, the MG63 cells were attached to all surfaces. Compared with the control surface, the cells were rounder and had a smaller adhesion area than the plasma treatment groups (Fig. 2). For RF-50W and RF-200W, actin filaments appeared at the edges of MG63 cells. On RF-200W, the MG63 cells are well spread and formed noticeable focal adhesions. Cells cultured on the control and DC-50W specimens showed few stress fibers, indicating limited interaction with the substrate (Fig. 2A,B). The actin filaments exhibited a flattened polygonal morphology spread over a wider area compared to control (Fig. 2C,D).

After 24 h, cells on the RF-50W and RF-200W specimens exhibited long extensions of cytoplasmic membranes, making the cells fully spreading out shape (Fig. 3C,D).

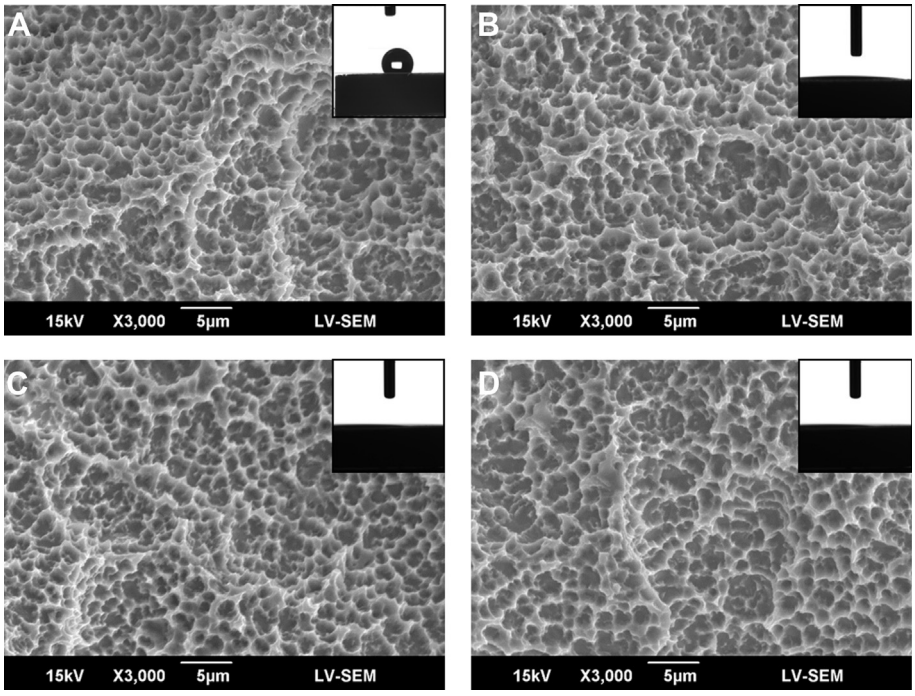

Figure 1 SEM morphology images of A. control (only SLA), B. DC-50W, C. RF-50W, and D. RF-200W. All specimens show mountain and valley structure with micron- and submicron-scale notches. Morphologies are the same but surface becomes hydrophilic after DC or RF plasma treatment.

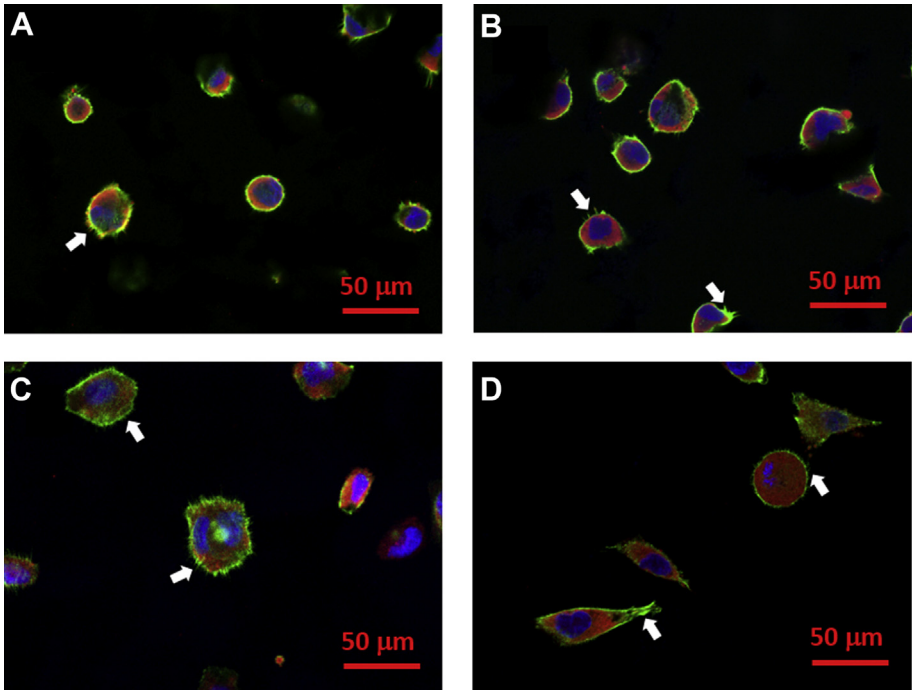

Figure 2 Fluorescence images of MG63 cells cultured on four types of surface after 1 h of incubation: A. control, B. DC-50W, C. RF-50W, and D. RF-200W. F-actin (green) was stained with Alexa Flour 488 phalloidin; vinculin (red) was stained with Alexa Fluor 594; nucleus (blue) was stained with DAPI. Actin filaments and vinculin expression are abundant after RF plasma treatment.

Vinculin-positive focal adhesions were observed in the cell plasma and elongated projections (Fig. 3C,D). The cell shape at 1 h (round) was different from that at 24 h (elongated) in all groups. The plasma treatment also induced the extension of the lamellipodia on RF-200W specimens (1 h vs. 24 h; Fig. 3C, white arrow).

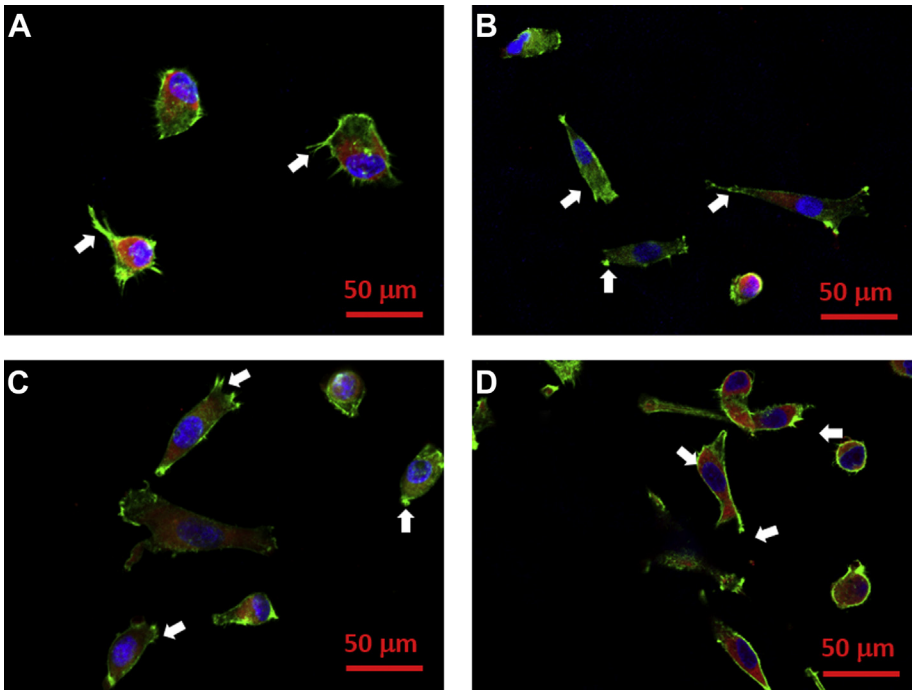

Figure 3 Fluorescence images of MG63 cells cultured on four types of surface after 24 h of incubation: A. control, B. DC-50W, C. RF-50W, and D. RF-200W. F-actin (green) was stained with Alexa Flour 488 phalloidin; vinculin (red) was stained with Alexa Fluor 594; nucleus (blue) was stained with DAPI. MG63 cells on RF-200W showed elongated morphology; cells in control group showed round morphology.

Bone-to-implant contact evaluation

At 8 weeks, the backscattered electron image of scanning electron microscopy (BEI-SEM) image of an RF-200W implant are shown in Fig. 4. Fig. 4 shows that bone tissues were ingrowth well on the thread of the implant. RF-200W implants displayed good direct bone-to-implant contact in most regions of the implant surfaces.

At 4 weeks (see Fig. 5B), there were statistically no significant differences between paired specimens (RF-200W, RF-50W) and (RF-50W, DC-50W); whereas the differences among all other specimen pairs were statistically significant. At 8 weeks, the BIC ratio of RF-200W showed highest value ($P < 0.05$). There was no significant different in BIC ratio among the control, DC50W, and RF-50W specimens.

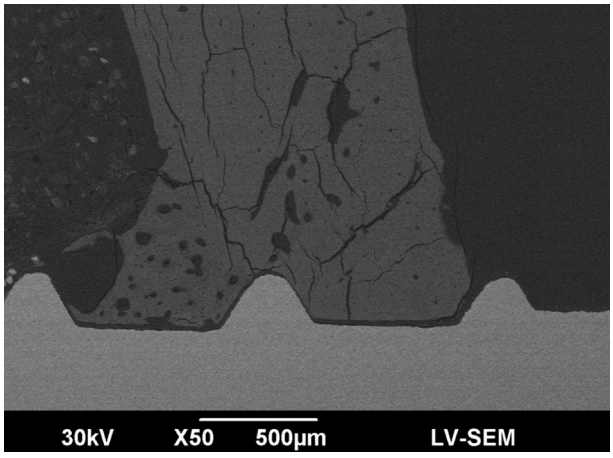

Figure 4 BEI-SEM image of RF-200W. New bone formation is dense and bone contact ratio is high at 8 weeks.

Discussion

The loading condition is positively correlate with good osseointegration. The osseointegration rate of titanium dental implants depends on implant composition and surface roughness. Previous studies reported that SLA treatment of implants leads to better bone healing at 4 or 6 weeks post-implantation than other treatments (polishing or only acid etching). The modSLA can improve bone healing thus shortening the healing time.[17–19] In this study, a rough surface with micron and submicron structures was created using the SLA method (Fig. 1). This plasma treatment did not affect surface roughness.[11] The roughness values for the four groups showed no statistically difference (Table 1). In addition, the functional OH groups on the SLA-roughened surface did not change the contact angle. These results are consistent with the previous research.[9,10,17,20] This implied that the functional OH groups had a great effect on wettability and thus enhanced the biological response. Most studies have end discussion in *in vitro* cell behavior, few continue to discuss the effect of OH groups *in vivo*.

In this study, the MG63 cells cultured on RF-50W and RF-200W exhibited more spreading (Fig. 2) compared to the control group. Plasma treatment can improve cell

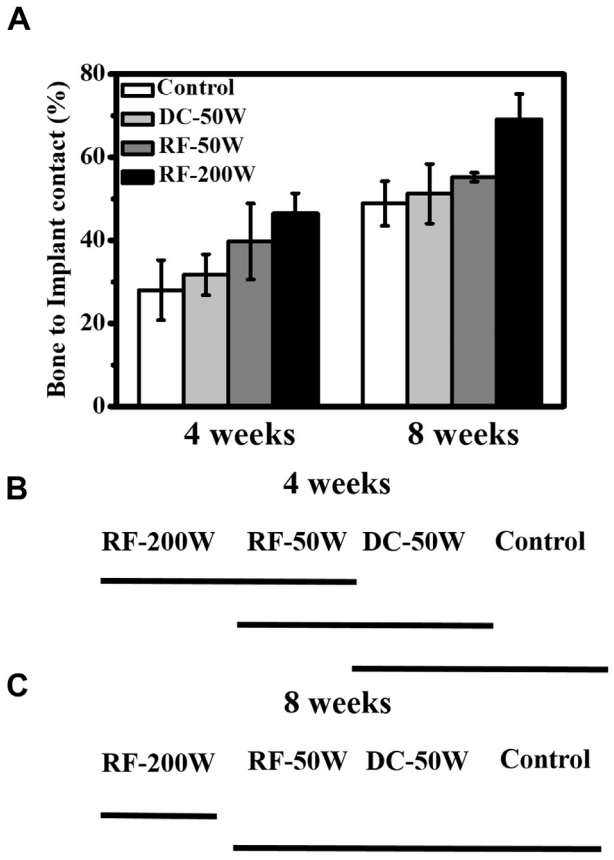

Figure 5 A. Bone-to-implant contact ratios after 4 and 8 weeks of healing. Bars labeled with underlines indicate significant difference between groups according to Duncan test ($n = 3$, $P < 0.05$). Duncan grouping of BIC at B. 4 weeks and C. 8 weeks.

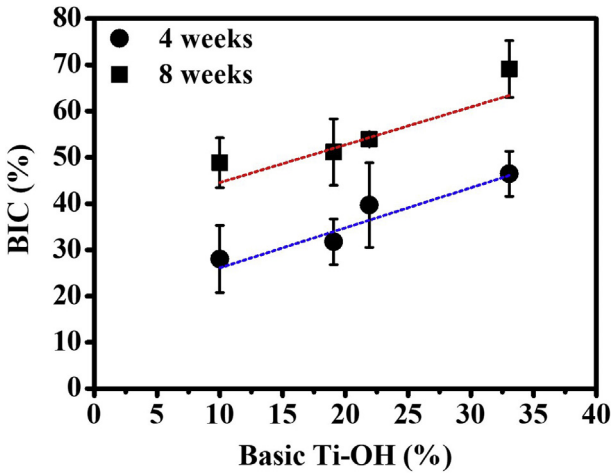

Figure 6 Effects of basic Ti—OH on BIC ratio. Increasing basic Ti—OH increased BIC ratios.

adhesion, particularly on the hydrophilic surface. The cytoskeletal organization, governs osteoblastic cell adhesion, may be influenced by a rough titanium surface.[21] Feng et al. reported that the basic hydroxyl $(OH)_b$ groups and the polar component are more important than the acidic hydroxyl $(OH)_a$ groups and the dispersion component of the total surface energy. Thus, $(OH)_b$ groups play a crucial role in osteoblast—titanium interaction.[8] Titanium surfaces with dissociated $(OH)_b$ groups have more positive charges. Previous studies reported that a high content of OH groups, a rough structure, and a charged surface can induce bone-related cells to express adhesion proteins, especially actin and vinculin.[22—24] The initial attachment of cells on the substrate is a key factor in biomaterial design and development.[25]

The protein adsorption of DC-50W and RF-50W are statistically different in our previous study shown in Table 1.[11] Cell behavior including cell attachment and spreading is strongly influenced by the protein adsorption. Fig. 2B,C showed attachment morphology containing actin filaments and there is more actin filaments of RF-50W than DC-50W at 1 h although the Ti—OH ratio showed no significant difference. The cell cytoskeleton was both flatter for RF-50W and RF-200W at 1 h but RF-200W expressed higher actin filaments on at 24 h. The *in vitro* cell response may be correlated with *in vivo* bone healing and regeneration. This means that good cell adhesion triggers subsequent responses, including new bone formation. Dense bone formation appeared on DC-50W, RF-50W, and RF-200W samples, indicating better osseointegration than the control. However, at 8 weeks, only RF-200W showed statistically difference (Fig. 5), which may be due to the different type of plasma treatment and plasma power. At both 4 and 8 weeks, there was a linear correlation between basic Ti—OH and the BIC ratio (Fig. 6).

In conclusion, plasma treatment was used to introduce functional OH groups on SLA-treated titanium surfaces without changing the surface topography and roughness. The abundant functional OH groups made the surface hydrophilic, enhancing cell adhesion and promoting the cytoskeleton to express focal adhesions. BIC analysis showed RF plasma treatment created surface with good cell affinity and *in vivo* examines more new bone formation than other groups. Furthermore, the abundant OH groups introduced by plasma treatments and basic Ti—OH groups had positive effects on BIC. Moreover, the basic Ti—OH showed a greater effect on bone regeneration. We propose that RF-plasma treatment can help to enhance bone healing at the early stage.

Conflicts of interest

The authors have no conflicts of interest relevant to this article.

Acknowledgments

This study was supported by the National Science Council, Taiwan (grant MOST 103-2622-E-006-045-CC2), and by Kaohsiung Medical University (KMU-KMUH Co-Project of Key Research, grant KMU-DK105005).

References

1. Wen B, Kuhn L, Charles L, et al. Comparison of bone morphogenetic protein-2 delivery systems to induce supracrestal bone guided by titanium implants in the rabbit mandible. *Clin Oral Implants Res* 2016;27:676—85.
2. Gehrke SA, Mate Sanchez de Val JE, Fernandez Dominguez M, et al. Effects on the osseointegration of titanium implants incorporating calcium-magnesium: a resonance frequency and histomorphometric analysis in rabbit tibia. *Clin Oral Implants Res* 2016: 1—7. https://doi.org/10.1111/clr.12909 [Epub ahead of print].
3. Contribunale JA, Puche RC. Osseointegration of titanium implants anodized with and without fluoride in the electrolyte. A study in rats. *Actual Osteol* 2017;13:46—57.
4. Gittens RA, McLachlan T, Olivares-Navarrete R, et al. The effects of combined micron-/submicron-scale surface roughness and nanoscale features on cell proliferation and differentiation. *Biomaterials* 2011;32:3395—403.
5. Buser D, Broggini N, Wieland M, et al. Enhanced bone apposition to a chemically modified SLA titanium surface. *J Dent Res* 2004;83:529—33.
6. Zhao G, Raines AL, Wieland M, et al. Requirement for both micron- and submicron scale structure for synergistic responses of osteoblasts to substrate surface energy and topography. *Biomaterials* 2007;28:2821—9.
7. Lopez-Heredia MA, Legeay G, Gaillard C. Radio frequency plasma treatments on titanium for enhancement of bioactivity. *Acta Biomater* 2008;4:1953—62.
8. Feng B, Weng J, Yang BC, et al. Characterization of surface oxide films on titanium and adhesion of osteoblast. *Biomaterials* 2003;24:4663—70.
9. Hu XX, Shen H, Shuai KG, et al. Surface bioactivity modification of titanium by CO2 plasma treatment and induction of hydroxyapatite: in vitro and in vivo studies. *Appl Surf Sci* 2011; 257:1813—23.
10. Guastaldi FP, Yoo D, Marin C, et al. Plasma treatment maintains surface energy of the implant surface and enhances osseointegration. *Int J Biomater* 2013;2013:1—6.
11. Chou WC, Wang RCC, Yang CY, Lee TM. Surface modification of direct-current and radio-frequency oxygen plasma treatments enhance cell biocompatibility. *Materials* 2017;10:1—17.
12. Canullo L, Genova T, Tallarico M, et al. Plasma of argon affects the earliest biological response of different implant surfaces: an in vitro comparative study. *J Dent Res* 2016;95:566—73.
13. MacDonald DE, Rapuano BE, Vyas P, et al. Heat and radiofrequency plasma glow discharge pretreatment of a titanium alloy promote bone formation and osseointegration. *J Cell Biochem* 2013;114:2363—74.
14. Branemark PI. Osseointegration and its experimental background. *J Prosthet Dent* 1983;50:399—410.
15. Yuan K, Chan YJ, Kung KC, Lee TM. Comparison of osseointegration on various implant surfaces after bacterial contamination and cleaning: a rabbit study. *Int J Oral Maxillofac Implants* 2014;29:32—40.
16. Lillie RD, Pizzolato P, Vacca LL. Salt Zenker, a stable, nonhemolytic, formaldehyde-free fixative - addition of salt to other acetic-acid fixatives. *Am J Clin Pathol* 1973;59:374—5.
17. Duske K, Koban I, Kindel E, et al. Atmospheric plasma enhances wettability and cell spreading on dental implant metals. *J Clin Periodontol* 2012;39:400—7.
18. Schlegel KA, Prechtl C, Most T, et al. Osseointegration of SLActive implants in diabetic pigs. *Clin Oral Implan Res* 2013; 24:128—34.
19. Park JW, Kwon TG, Suh JY. The relative effect of surface strontium chemistry and super-hydrophilicity on the early osseointegration of moderately rough titanium surface in the rabbit femur. *Clin Oral Implants Res* 2013;24:706—9.
20. Tseng WY, Hsu SH, Huang CH, et al. Low pressure radiofrequency oxygen plasma induced oxidation of titanium - surface characteristics and biological effects. *PLoS One* 2013;8: 1—8.
21. Salido M, Vilches JI, Gutierrez JL, Vilches J. Actin cytoskeletal organization in human osteoblasts grown on different dental titanium implant surfaces. *Histol Histopathol* 2007;22: 1355—64.
22. Vidal G, Blanchi T, Mieszawska AJ, et al. Enhanced cellular adhesion on titanium by silk functionalized with titanium binding and RGD peptides. *Acta Biomater* 2013;9:4935—43.
23. Liu YT, Lee TM, Lui TS. Enhanced osteoblastic cell response on zirconia by bio-inspired surface modification. *Colloids Surf B Biointerfaces* 2013;106:37—45.
24. Baharloo B, Textor M, Brunette DM. Substratum roughness alters the growth, area, and focal adhesions of epithelial cells, and their proximity to titanium surfaces. *J Biomed Mater Res* 2005;74(1):12—22.
25. D'Arcangelo E, McGuigan AP. Micropatterning strategies to engineer controlled cell and tissue architecture in vitro. *Biotechniques* 2015;58:13—23.